*Proc. of the European Safety and Reliability Conference (ESREL 2026)*
*Edited by* José C. Matos, Paulo B. Lourenço, Michael Beer, Daniel Oliveira,
Edoardo Patelli, Hélder S. Sousa, Rui A. Silva and Monica Santamaria
 *Published by* Research Publishing, Singapore.
doi: 10.3850/ESREL2026061419_esrel26-p26263-cd

# Modeling Societal Consequences of Damage Cascades in Critical Infrastructures to Quantify Resilience Benefits of Nature-Based Solutions

Benjamin Lickert, Mirjam Fehling-Kaschek, Ivo Häring, Alexander Stolz
*Fraunhofer Ernst-Mach-Institute, EMI, Efringen-Kirchen, Germany*
E-mail: {*benjamin.lickert; mirjam.fehling-kaschek; ivo.haering; alexander.stolz*}*@emi.fraunhofer.de*

Modern societies rely on intricate critical infrastructure networks to satisfy essential needs. Quantifying and characterizing their resilience is crucial for pinpointing vulnerabilities that may interrupt operations and for judging mitigation measures that enhance crisis preparedness, prevention, response, or recovery. Nature-based solution (NBS) approaches have recently attracted attention in this context. To evaluate their efficacy against adverse events under varied initial conditions and disaster intensities, robust modeling frameworks are necessary. Prior studies introduced a graph-based modeling framework that offers a comprehensive view of the resilience of critical infrastructures during natural disasters, notably flash floods, via simulations of cascading failures and subsequent recovery phases. Based on this foundation, this paper presents an approach to simulate the societal consequences of such failures to widen the understanding of disaster consequences. Key services provided by critical infrastructures are identified and a process model is developed that captures the local population's demand for each service, e.g., hospital treatments or cash provision by ATMs. Once a natural disaster occurs, these demands may increase while the critical infrastructures are impaired by disaster effects. In consequence, service-specific backlogs emerge that depend on the disaster and local vulnerabilities. Inspecting exemplary simulation results, this paper shows how such estimations can be used to assess NBS mitigated and unmitigated floods.

*Keywords*: resilience quantification, societal consequences, cascading failure modeling, critical infrastructure, natural disasters, nature-based solutions

## 1. Introduction

Critical infrastructures (CIs) form the backbone of modern societies. Understanding und quantifying CI resilience is essential to detect and assess operational risks and potential failure cascades Thoma et al. (2016); Häring et al. (2021); Stolz et al. (2024); Fischer and Stolz (2026). Quantifying the impact of mitigation options is of equal importance to support planning and prioritization.

Regarding such mitigation options, Nature-Based Solutions (NBSs) are attracting more and more attention recently (Van den Bosch and Sang (2017); Lafortezza et al. (2018)) due to current developments (e.g., climate change, ecosystem degradation). NBSs promise to strengthen (critical) infrastructure resilience while delivering environmental co-benefits. The European research project NBSInfra[a] advances NBS integration in urban settings to strengthen CI resilience to climate-related threats, such as flooding.

Given that real-world deployments remain limited and empirical evidence on NBS performance against natural hazards is scarce, modeling and simulation is vital to assess protective effects on CIs across diverse disruptions and initial conditions. Prior work employed graph-, flow-, and agent-based models, as well as hybrids (see Ouyang (2014)), to represent infrastructures and their interdependencies. These models enable scenario analyses across spatial scales and time horizons but many studies still target single CI sectors and overlook dynamic processes — e.g., time-evolving damage cascades — constraining system-wide, holistic assessments of CI network resilience. Additionally, related work on interdependent CI modeling often focuses on physical service continuity, while fewer studies connect CI functionality trajectories to population-level service accessibility and demand backlogs during response phases. Queuing and agent-based approaches have been used to represent emergency

[a] https://nbsinfra.eu/

demand surges and constrained service capacities, but are rarely coupled to dynamic cascade models that capture delayed failures and recovery. Our approach presented below bridges this gap by linking cascade-driven functionality time series to a process-based demand and capacity model in a unified simulation. It is based on prior work Fehling-Kaschek et al. (2025); Lickert et al. (2025) that demonstrated the use of graph-based modeling to analyze and quantify the temporal evolution of failure cascades in interdependent critical infrastructure networks.

Building upon these results, this paper presents a method to simulate the societal impacts of cascading CI failures. We identify key services provided by critical infrastructures and develop a process-based model that captures local population demand for different services (e.g., ambulance services) across distinct disaster-response phases. The paper contributes (i) a coupling approach that maps time-dependent CI functionality trajectories from cascade simulations to service-specific capacity processes, (ii) a demand-generation model that represents citizens' service requests and quantifies unmet demand as backlog over time, and (iii) an illustrative comparison of unmitigated versus NBS-mitigated flood scenarios for the Aveiro City-Lab from NBSInfra, demonstrating how NBS effects propagate from reduced direct damages to reduced societal service backlogs. The proposed framework is generic with respect to hazard type and CI portfolio, requiring only CI service-to-capacity mappings and a phase-specific demand parameterization.

## 2. Study Region and Cascade Modeling

For the following studies, we inspect the NBSInfra City-Lab of Aveiro. The city faces high risk of flash flooding due to combined fluvial and estuarine dynamics from its lagoon. The lack of mitigation of peak hydrographic flows leads to severe risks regarding the flooding of urban and agricultural areas. NBSs considered in NBSInfra to improve the situation are predominantly related to rehabilitation of water streams and the construction and upgrading of water retention capacities. For more information on Aveiro see Fehling-Kaschek et al. (2025).

The cascade modeling for Aveiro employs the CaESAR simulation framework, developed by Fraunhofer EMI and applied in numerous resilience assessments of critical infrastructures, e.g., telecommunication, airports, gas networks, and power outages Lickert et al. (2024). The simulation requires a graph model of local infrastructures with nodes (e.g., hospitals, power supply) and edges encoding interdependencies. An adverse event is specified via a threat definition file that can stochastically damage entities or areas. Following this adverse event, the interdependencies among system components may trigger cascades causing additional failures, while repair mechanisms drive the recovery of failed elements. A stepwise simulation of the event and the subsequent period of cascading damage and repair produces a trajectory of the network's performance.

The selection of nodes for the network model of Aveiro constructed and inspected in Fehling-Kaschek et al. (2025); Lickert et al. (2025) followed the European Commission's list of critical sectors Commission of the European Communities (2005) that encompasses energy, transport, communication technology, water, food, health, finance, public/legal order and safety, civil administration, chemical/nuclear, and space/research. Critical services and facilities were extracted from OpenStreetMap via Overpass Turbo[b]. The study area, encompassing the southern half of the Aveiro district, includes zones that are prone to flash floods as well as adjacent regions to capture mutual support (e.g., rerouting patients to nearby hospitals).

For the work presented in this paper, the network was refined by including information provided by the municipality of Aveiro. This allowed to correct wrong, outdated or missing information from OpenStreetMap. In particular, the sets of nodes representing the low voltage power grid, ambulance services, the water grid, banks and ATMs were adjusted. Additionally, additional infrastructure (not necessarily critical but still relevant) was added to the model. Here, eight pharma-

[b] https://overpass-turbo.eu

cies (dependent on the nearest low voltage node), 89 public places (independent of any other network node), 13 schools, 68 public buildings (both categories dependent on the nearest low voltage and water nodes), and 19 water sewage facilities (dependent on the nearest low voltage node) were added. Figure 1 shows at the top the full resulting model network with 966 nodes and 2104 edges.

To identify network nodes susceptible to flooding, openly available elevation data was examined Lickert et al. (2025). QGIS[c] was used to extract the Copernicus Digital Elevation Model (DEM) at a resolution of 30 m European Space Agency (2024) for the Aveiro region via OpenTopography. The dataset was analyzed to delineate low-lying areas near the coastline downstream of the Aveiro river. Figure 1 second panel shows the City of Aveiro's network nodes in red with elevations below 18 m. It is assumed that these low-lying nodes will be damaged during a severe flash flood event. The repair time $t_{R,i}$ of direct flood damages is set to one week. To estimate the effects of NBS flood mitigation measures, like the de-sealing of surfaces, a mitigated flood event is considered as well. For this case, it is assumed that only very low lying nodes with elevations below 6 m are damaged by the flood. These nodes can be seen in the bottom panel of Fig. 1. We observe that they cluster near the river course (marked in blue), also supporting the validity of the identification approach based on elevation information.

We note that the elevation thresholds (18 m for severe flooding and 6 m for mitigated flooding) are used as a proxy for flood exposure in the absence of detailed hydrodynamic simulations. They were selected to (i) capture low-lying coastal and lagoon-adjacent areas visible in the DEM and (ii) produce a plausible fraction of directly affected assets consistent with historic flood-prone zones. We emphasize that these thresholds represent scenario definitions rather than calibrated hazard intensities. A sensitivity analysis varying the thresholds is planned as future work to quantify robustness of the resulting service backlogs.

Figure 2 shows the results of the cascade simulations for both flood scenarios. Solid lines account for the severe flood, while dashed lines represent the mitigated flood event. The infrastructures depicted are used for the modeling of societal consequences in the next section. Most of them exhibit delayed decays, which result from the assumption that they can continue operating for some time in emergency mode without their critical dependencies being served externally before shutting down, see Lickert et al. (2025).

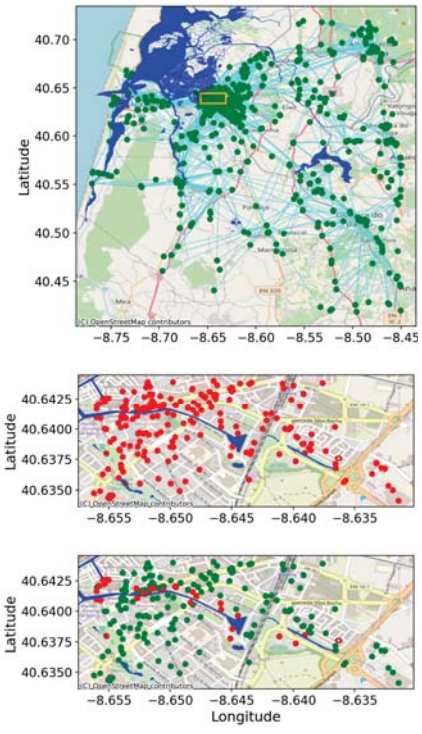


Fig. 1. Network of critical infrastructures for the Aveiro region and its surrounding. Top, the full network is shown, the orange box indicates the identical position of the panels shown below. Here, the nodes targeted by the severe flash flood event are shown in red (middle panel), the nodes damaged by the mitigated flood event (bottom panel) are also marked in red while the green dots represent the nodes which stay intact compared to the severe flash flood.

## 3. Modeling Societal Consequences

While it is useful to estimate the range and severity of flood damages in the local CI network, it

[c]https://qgis.org/

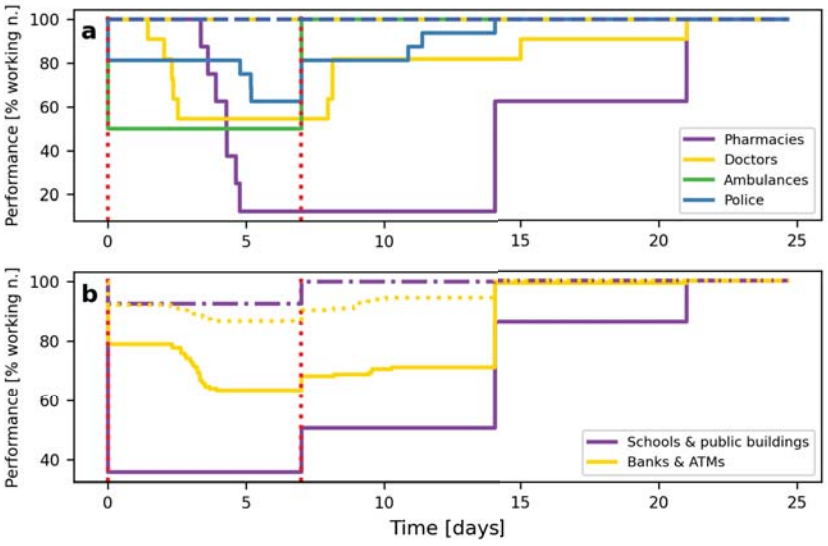


Fig. 2. Effects of the severe flash flood event (solid lines) and the mitigated flood event (dashed lines) on (critical) infrastructures that are further inspected for the modeling of societal consequences. The events take place at Time = 0 d (first red vertical line), the repair of the flood damages takes one week (second red vertical line) at Time = 7 d.

does not capture the full picture of the disaster's consequences. This section presents an approach to simulate the societal consequences of the CI failures caused by the severe and mitigated floods shown in Fig. 2. The process model is implemented using the SimPy package in Python. It has three main pillars: (i) a representation of the services in the region/city under study, (ii) a representation of the demands of the local population for the services and (iii) generators of these demands.

We use the fraction of operational nodes per CI category as a parsimonious proxy for functionality. This choice reduces data requirements but does not reflect heterogeneous asset capacities (e.g., large vs. small hospitals). Currently, we partly address this by translating operational node counts into service capacity via sector-specific scaling factors (Eqs. 1 - 6). Future work will replace node fractions by capacity-weighted functionality metrics where asset-level capacity data are available.

### 3.1. *Representation of the Services*

The region under study, in this paper Aveiro and its surrounding, is implemented as python class using SimPy containers to represent the capacities of the different services. The services considered by the modeling are (i) access to medicine via pharmacies, (ii) access to medical care via resident doctors, (iii) access to emergency care via ambulances, (iv) access to cash via banks and ATMs and (v) access to municipal disaster support via schools and public buildings. For the latter it is assumed that both building types are used during disasters to support the local population.

The capacities of the first four services (medicine, medical care, emergency care, and police) are represented by slots, where each slot can be occupied by one citizen for a certain period of time (see next subsection). The numbers of available slots $S(t)$ at time $t$ are based on the numbers of operative nodes $N_{\mathrm{pharm}}(t)$, $N_{\mathrm{doc}}(t)$, $N_{\mathrm{amb}}(t)$, and $N_{\mathrm{pol}}(t)$ as predicted by the cascade simulation, see Fig. 2a. The scaling factors in Eqs. 1 to 4 represent average parallel service channels per facility (e.g., counters or staff teams) and were set to produce plausible utilization levels for the illustrative scenario in Section 4.

$$S_{\mathrm{medicine}}(t) = 3 \cdot N_{\mathrm{pharm}}(t), \qquad (1)$$

$$S_{\text{medcare}}(t) = 2 \cdot N_{\text{doc}}(t), \tag{2}$$

$$S_{\text{emerg}}(t) = 4 \cdot N_{\text{amb}}(t), \tag{3}$$

$$S_{\text{pol}}(t) = 2 \cdot N_{\text{pol}}(t). \tag{4}$$

At each time step, the simulation checks for each service whether the number of operational nodes has decreased or increased. If it decreases, the overall number of respective slots $S(t)$ is reduced according to the equations above by sequentially removing slots. If a slot cannot be removed immediately because it is occupied, it is removed as soon as the citizen releases it. If the number of operational nodes increases, $S(t)$ is increased immediately according to the equations above.

The other two services, disaster support and cash access, are defined differently. Here, the citizens consume "units" $U(t)$ of both services, e.g., Euros in case of the cash service. The stocks of both services are periodically refilled, the number of refilled "units" depends on the numbers of operative nodes $N_{\text{school}}(t)$ and $N_{\text{pub.build.}}(t)$ for disaster support, and on $N_{\text{bank}}(t)$ and $N_{\text{ATM}}(t)$ for cash supply as predicted by the cascade simulation (see Fig. 2b). For the simulation shown in Section 4, we assume

$$U_{\text{support}}(t) = U_{\text{support}}(t - \Delta t) + 4 \cdot N_{\text{school}}(t) + 8 \cdot N_{\text{pub.build}}(t) \tag{5}$$

with a refilling time step $\Delta t = 1$h and

$$U_{\text{cash}}(t) = U_{\text{cash}}(t - \Delta t) + 22000 \cdot N_{\text{bank}}(t) + 12000 \cdot N_{\text{ATM}}(t) \tag{6}$$

with a refilling time step $\Delta t = 24$h. The refill amounts in Eqs. 5 and 6 approximate periodic replenishment under constrained logistics (hourly for municipal support, daily for cash). Both services employ in addition fixed capacity limits that account for, e.g., the maximum amount of cash an ATM can hold.

Since empirical local data were not available, the scaling factors in Eqs. 1 - 6 should be interpreted as scenario assumptions; Section 4, therefore focuses on relative differences between severe and mitigated flooding rather than absolute service levels.

### 3.2. *Representation of Demand*

The demand of the local population for the six services in the simulation is modeled through individual "citizen processes". Each process, when generated, represents a single citizen demanding exactly one service $x$. For example, a citizen process may request one slot from $S_{\text{medicine}}(t)$ or a certain amount of cash from $U_{\text{cash}}(t)$, but never both simultaneously. It is furthermore assumed that a citizen process generated at simulation time $t = t_0$ appears in one of three disaster response phases $p \in [1, 2, 3]$ representing early, mid and late phase of the disaster response cycle. Each citizen process has:

- A maximal waiting time $t_{\text{wait}}(p, x)$ that represents the time the citizen can (or wants to) wait for the requested service $x$ in the current disaster response phase $p$.
- A slot occupation time $t_{\text{occ}}$ drawn from the value range $[t_{\text{occ}}^{\min}(p, x), t_{\text{occ}}^{\max}(p, x)]$ that represents the time the process occupies one of the slots of service $x$ in eqn. 1 to 4 or
- a unit demand $d$ drawn from the value range $[d^{\min}(p, x), d^{\max}(p, x)]$ representing the units requested from service $x$ of eq. 5 or 6.

If the requested service is not provided within $t_{\text{wait}}$, the request is canceled. In our model, a canceled request represents a service need that could not be met locally within the assumed tolerance window and had to be substituted by alternative means (e.g., traveling outside the region). Hence, "unsatisfied demand" is interpreted as a proxy for societal disruption and loss of accessibility rather than as direct harm. A systematic categorization and analysis of these disruptions is beyond the scope of this paper and is left for future work.

### 3.3. *Generation of Demand*

Citizen processes for all six services are generated using service-specific inter-arrival times. This indicates that after the $i$-th process for service $x$ is instantiated, the next process of type $x$ is scheduled after the time $t_{\text{gen},x,i}$ drawn from the window $[\, t_{\text{gen},x}^{\min},\, t_{\text{gen},x}^{\max}\,]$. Furthermore, it is assumed that these time windows depend on the current disaster-response phase $p$.

## 4. Exemplary Simulation Results

With the simulation setup defined, we now examine exemplary results using the damage cascades in Fig. 2 for the severe and mitigated flash floods. The parameters for the citizen processes and the demand generation are specified in Tabs 1 and 2. Although parameters were chosen for illustrative purposes, we ensured internal plausibility by (i) selecting inter-arrival times that yield realistic order-of-magnitude request volumes for a mid-sized urban area and (ii) setting $t_{\mathrm{wait}}$ values to reflect urgency differences across response phases (highest urgency in Phase 1). The study therefore emphasizes comparative insights (severe vs. mitigated) rather than absolute predictions. To isolate the effect of reduced flood damages on disaster response, the same parameters were used for both floods. We acknowledge that this assumption does not reflect all aspects of real-world conditions, as successful flood mitigation would likely lower the demand for some services in certain phases of the disaster response, such as emergency medical services.

Regarding the disaster response, the early phase (Phase 1) spans the first two days after the flash flood. Phase 2 covers the subsequent five days, i.e., Phases 1 and 2 coincide with the period of repairing flood damages in the cascade simulation shown in Fig. 2. Phase 3 represents the aftermath of the disaster and the transition back to normal conditions. The peak of $t_{\mathrm{wait}}$ values in Phase 2 reflects our assumption that demand in Phase 1, e.g., medical needs, is more urgent than in Phase 2, as the immediate effects on the population must be addressed first. Conversely, as society transitions back to normal conditions (Phase 3), citizens' patience is assumed to diminish, combining fatigue with improved opportunities to obtain services outside the local region, such that $t_{\mathrm{wait}}$ is significantly reduced. Cash services are an exception. They are not assumed to be an immediate priority when the disaster strikes (Phase 1), however, they become more urgent in Phase 2 due to potential disruptions to digital payments, and then decline in urgency again in Phase 3.

The other model parameters, $t_{\mathrm{occ}}$ and $d$ in Tab. 1 and $t_{\mathrm{gen}}$ in Tab. 2, follow the same reasoning. Figure 3 shows the temporal evolution of free capacities for selected services under the severe and mitigated flood scenarios. For medicine and medical care, both scenarios behave similarly in Phase 1 but diverge significantly in Phases 2 and 3, reflecting the consequences of the cascading failures in the severe case. Support services exhibit capacity constraints in Phase 1 for both scenarios,

Table 1. Parameters of the citizen processes used for the simulation results. All times are given in (min).

| Service | Phase | $t_{\mathrm{wait}}$ | $t_{\mathrm{occ}}$ | $d$ |
|---|---|---|---|---|
| Medicine | 1 | 180 | [15, 45] | – |
| | 2 | 240 | [5, 20] | – |
| | 3 | 60 | [5, 15] | – |
| Med. care | 1 | 240 | [15, 35] | – |
| | 2 | 360 | [10, 30] | – |
| | 3 | 90 | [10, 30] | – |
| Emergency | 1 | 120 | [60, 90] | – |
| | 2 | 180 | [45, 60] | – |
| | 3 | 60 | [60, 120] | – |
| Police | 1 | 300 | [30, 60] | – |
| | 2 | 480 | [20, 40] | – |
| | 3 | 240 | [30, 45] | – |
| Support | 1 | 660 | – | [5, 10] |
| | 2 | 780 | – | [3, 8] |
| | 3 | 300 | – | [1, 3] |
| Cash | 1 | 660 | – | [500, 1000] |
| | 2 | 180 | – | [1000, 2500] |
| | 3 | 700 | – | [700, 1500] |

Table 2. Time windows in (min) for the inter-arrival times $t_{\mathrm{gen}}$ of the different services for all three disaster response phases.

| Service | Phase 1 | Phase 2 | Phase 3 |
|---|---|---|---|
| Medicine | [1.2, 3.5] | [1.5, 4] | [8, 15] |
| Med. care | [0.7, 1.8] | [1.5, 4] | [8, 20] |
| Emergency | [5, 10] | [20, 40] | [40, 120] |
| Police | [5, 10] | [10, 20] | [20, 40] |
| Support | [0.5, 1] | [0.5, 1.5] | [1.5, 3] |
| Cash | [3, 6] | [0.6, 1] | [0.5, 1.5] |

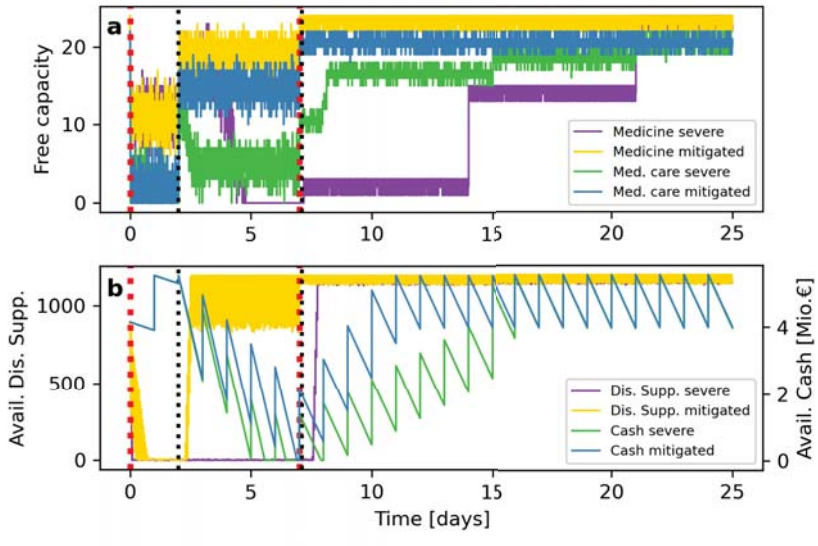


Fig. 3. Available capacity of medicine and medical care services in units of slots (a) and available disaster support units and cash (b). Results for the severe and the mitigated flood are shown. Vertical lines indicate the duration of the repair of flood damages (red) and the disaster response phases (black).

however, Phase 2 is no longer critical in the mitigated case. For the cash service, reserves decline in Phase 2 in both scenarios due to increased demand during this phase.

To quantify societal consequences, we can inspect the cumulative numbers of canceled requests/unmet demand (backlog) per service over time due to exceeding $t_{\text{wait}}$ since they directly reflect the mismatch between supply and demand during response phases. Despite capacity constraints in Phase 1, medical care demand is fully met throughout the simulation for both floods (Fig. 4). In contrast, medicine services exhibit unsatisfied demand at the end of Phase 2, indicating that disaster effects can manifest with a substantial delay relative to the causal incident. This behavior is explained by the delayed failure of pharmacies (see Fig. 2). In contrast, the unsatisfied demand for cash services, which also emerges at the end of Phase 2, is primarily driven by increased demand during this phase. The most pronounced shortcomings occur for support services, with unsatisfied demand in Phases 1 and 2 under the severe flood scenario. For the mitigated flood scenario, no service exhibits unmet demand in any phase.

## 5. Conclusion

This paper introduced an approach to model the societal consequences of failure cascades in CI triggered by natural disasters. The method was illustrated with exemplary simulations for a model of the Aveiro region under two flash flood scenarios, one without and one with NBS resilience improvements. NBS effects are represented here by a reduced set of directly flooded assets, i.e., a shift in the exposure scenario. This abstraction captures a first-order protective effect but does not model hydrodynamic mechanisms or partial damage states. Future work will link NBS interventions to hazard intensity fields (e.g., depth/velocity) from hydraulic models. The assumed reduced flooding of CI nodes was shown to reduce the societal effects of flash floods in all resilience cycle phases.

Because the parameter calibration was designed for illustrative purposes and simplifying assumptions - such as fixed demand across scenarios - were applied, future work should refine the model

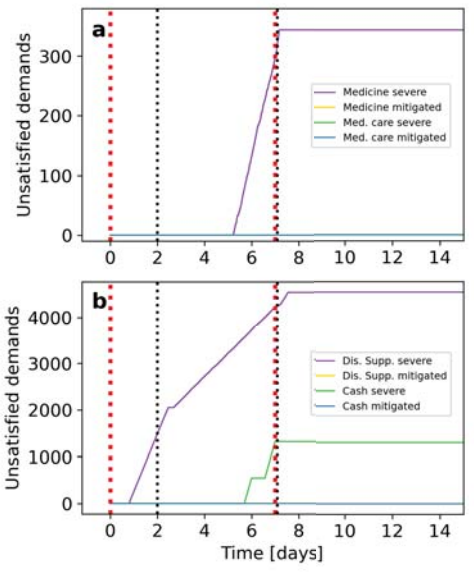


Fig. 4. Unsatisfied demands for medicine and medical care services (a) and for support and cash (b). Results for both flood scenarios are shown. Vertical lines indicate the duration of the repair of flood damages (red) and the disaster response phases (black). Note for (a) that the blue line covers all lines but violet, i.e. only the medicine demand is not covered in the severe flooding scenario. For (b), the blue line covers the red one.

calibration. In addition, the set of considered societal services needs to be expanded and the framework should be applied to further study regions and disaster types.

**Acknowledgement**

This work is funded by the project No. 101121210 "CityNature-Based Solutions Integration to Local Urban Infrastructure Protection for a Climate Resilient Society" (NBSINFRA) from the European Union's Horizon 2022 program. Funded by the European Union. Views and opinions expressed are, however, those of the author(s) only and do not necessarily reflect those of the European Union or REA. Neither the European Union nor the granting authority can be held responsible for them.

## References

Commission of the European Communities (2005). Green paper on a European program for critical infrastructure protection. Page 24, Accessed: 09/01/2025.

European Space Agency (2024). Copernicus global digital elevation model. Distributed by OpenTopography. Accessed: 09/01/2025.

Fehling-Kaschek, M., B. Lickert, A. Stolz, E. Teixeira, A. Zarghami, L. Connolly, M. Cullinane, M. Monroy, and R. Borg (2025). Resilience quantification for critical infrastructure in urban areas including nature-based solutions. In E. B. Abrahamsen, T. Aven, F. Bouder, R. Flage, and M. Ylönen (Eds.), *Proceedings of the 35th European Safety and Reliability Conference (ESREL 2025) and the 33rd Society for Risk Analysis Europe Conference (SRA-E 2025)*, pp. 758–765.

Fischer, S. G. and A. Stolz (2026). Quantitative assessment of crises via central moments. *Reliability Engineering & System Safety 265*, 111472.

Häring, I., M. Fehling-Kaschek, N. Miller, K. Faist, S. Ganter, K. Srivastava, A. K. Jain, G. Fischer, K. Fischer, J. Finger, et al. (2021). A performance-based tabular approach for joint systematic improvement of risk control and resilience applied to telecommunication grid, gas network, and ultrasound localization system. *Environment Systems and Decisions 41*, 286–329.

Lafortezza, R., J. Chen, C. K. van den Bosch, and T. B. Randrup (2018). Nature-based solutions for resilient landscapes and cities. *Environmental Research 165*, 431–441.

Lickert, B., M. Fehling-Kaschek, and A. Stolz (2025). Assessing the benefits of nature-based solutions by modelling damage cascades in critical infrastructures. In *Life-Cycle Performance of Structures and Infrastructure Systems in Diverse Environments*, pp. 1795–1802. CRC Press.

Lickert, B., K. Srivastava, K. Schroven, M. Fehling-Kaschek, and A. Stolz (2024). Modeling impact of power outages on interdependent critical infrastructure. In *Proceedings of the 34th European Safety and Reliability Conference (ESREL)*.

Ouyang, M. (2014). Review on modeling and simulation of interdependent critical infrastructure systems. *Reliability engineering & System safety 121*, 43–60.

Stolz, A., J. H. Tang, S. G. Fischer, and K. Fischer (2024). A rheological model analog for assessing the resilience of socio-technical systems across sectors. *Environment Systems and Decisions*, 1–24.

Thoma, K., B. Scharte, D. Hiller, and T. Leismann (2016). Resilience engineering as part of security research: Definitions, concepts and science approaches. *European Journal of Security Research 1*, 3–19.

Van den Bosch, M. and Å. O. Sang (2017). Urban natural environments as nature based solutions for improved public health – a systematic review of reviews. *Environmental Research 158*, 373–384.